

AD

TECHNICAL REPORT ARCCB-TR-03006

**EXPERIMENTAL DATA, NUMERICAL FIT, AND FATIGUE  
LIFE CALCULATIONS RELATING TO THE BAUSCHINGER  
EFFECT IN HIGH-STRENGTH ARMAMENT STEELS**

**EDWARD TROIANO  
ANTHONY P. PARKER  
JOHN UNDERWOOD  
CHARLES MOSSEY**

**APRIL 2003**



**US ARMY ARMAMENT RESEARCH,  
DEVELOPMENT AND ENGINEERING CENTER**  
Close Combat Armaments Center  
Benét Laboratories  
Watervliet, NY 12189-4000



**APPROVED FOR PUBLIC RELEASE; DISTRIBUTION UNLIMITED**

**20030610 055**

## **DISCLAIMER**

The findings in this report are not to be construed as an official Department of the Army position unless so designated by other authorized documents.

The use of trade name(s) and/or manufacturer(s) does not constitute an official endorsement or approval.

## **DESTRUCTION NOTICE**

For classified documents, follow the procedures in DoD 5200.22-M, Industrial Security Manual, Section II-19, or DoD 5200.1-R, Information Security Program Regulation, Chapter IX.

For unclassified, limited documents, destroy by any method that will prevent disclosure of contents or reconstruction of the document.

For unclassified, unlimited documents, destroy when the report is no longer needed. Do not return it to the originator.

REPORT DOCUMENTATION PAGE			Form Approved OMB No. 0704-0188	
Public reporting burden for this collection of information is estimated to average 1 hour per response, including the time for reviewing instructions, searching existing data sources, gathering and maintaining the data needed, and completing and reviewing the collection of information. Send comments regarding this burden estimate or any other aspect of this collection of information, including suggestions for reducing this burden, to Washington Headquarters Services, Directorate for Information Operations and Reports, 1215 Jefferson Davis Highway, Suite 1204, Arlington, VA 22202-4302, and to the Office of Management and Budget, Paperwork Reduction Project (0704-0188), Washington, DC 20503.				
1. AGENCY USE ONLY (Leave Blank)	2. REPORT DATE April 2003	3. REPORT TYPE AND DATES COVERED Final		
4. TITLE AND SUBTITLE EXPERIMENTAL DATA, NUMERICAL FIT, AND FATIGUE LIFE CALCULATIONS RELATING TO THE BAUSCHINGER EFFECT IN HIGH-STRENGTH ARMAMENT STEELS		5. FUNDING NUMBERS AMCMS No. 6226.24.H180.0 PRON No. TU2		
6. AUTHORS Edward Troiano, Anthony P. Parker (Royal Military College of Science, Cranfield University, Swindon, UK), John Underwood, and Charles Mossey				
7. PERFORMING ORGANIZATION NAME(S) AND ADDRESS(ES) U.S. Army ARDEC Benet Laboratories, AMSTA-AR-CCB-O Watervliet, NY 12189-4000		8. PERFORMING ORGANIZATION REPORT NUMBER ARCCB-TR-03006		
9. SPONSORING / MONITORING AGENCY NAME(S) AND ADDRESS(ES) U.S. Army ARDEC Close Combat Armaments Center Picatinny Arsenal, NJ 07806-5000		10. SPONSORING / MONITORING AGENCY REPORT NUMBER		
11. SUPPLEMENTARY NOTES Presented at Gun Tubes Conference 2002, Keble College, Oxford, UK, 15-18 September 2002. Published in <i>ASME Journal of Pressure Vessel Technology</i> .				
12a. DISTRIBUTION / AVAILABILITY STATEMENT Approved for public release; distribution unlimited.		12b. DISTRIBUTION CODE		
13. ABSTRACT (Maximum 200 words) The uniaxial Bauschinger effect has been evaluated in several high-strength steels being considered for armament use. Tests were conducted at plastic strains up to 3.5%. Results of testing show a progressive decrease in Bauschinger effect up to plastic strains of approximately 1% (for all materials investigated), after which there is little further decrease. Several key features were discovered during testing. First, all of the materials tested exhibited a changing modulus, where the elastic modulus on unloading after tensile plastic straining is consistently lower than that observed in the original loading of the specimens. The amount of modulus reduction depends upon the material tested, and larger reductions are observed with increasing amounts of tensile plastic strain. Prior work by Milligan et al., reported Bauschinger effect factor, $\beta$ , for a modified 4340 steel (old vintage A723 steel), which compares well with the present work. However their results failed to mention any modulus reduction. Secondly the expected strength reduction was seen where a reduced compressive strength is observed as a result of prior tensile plastic straining. Numerical curve fits used to calculate residual stresses, which take into account both the modulus reduction and strength reduction, are presented for all materials. Fatigue life calculations, utilizing the numerical curve fits, show good agreement with full size A723 laboratory fatigue test results.				
14. SUBJECT TERMS Bauschinger Effect Factor, Bauschinger Modulus Reduction (BMR), Bauschinger Strength Reduction (BSR), Fatigue Life, High-Strength Armament Steels			15. NUMBER OF PAGES 14	16. PRICE CODE
17. SECURITY CLASSIFICATION OF REPORT UNCLASSIFIED	18. SECURITY CLASSIFICATION OF THIS PAGE UNCLASSIFIED	19. SECURITY CLASSIFICATION OF ABSTRACT UNCLASSIFIED	20. LIMITATION OF ABSTRACT UL	

NSN 7540-01-280-5500

Standard Form 298 (Rev. 2-89)  
Prescribed by ANSI Std. Z39-1  
298-102

AQM03-08-2078

## TABLE OF CONTENTS

	<u>Page</u>
INTRODUCTION .....	1
EXPERIMENTAL BAUSCHINGER TEST RESULTS .....	2
Bauschinger Modulus and Strength Reduction .....	3
Comparison to Milligan Data .....	5
Modulus Recovery .....	5
ANALYSIS OF RESIDUAL STRESSES/NUMERICAL FIT OF THE BAUSCHINGER EFFECT .....	6
FATIGUE LIFE APPROXIMATION .....	7
CLOSING REMARKS .....	10
REFERENCES .....	12

### TABLES

1. Bauschinger Test Data .....	4
2. Bauschinger Scaling Factor Constants .....	7
3. Paris Law Coefficients and Exponents .....	8

### LIST OF ILLUSTRATIONS

1. Typical uniaxial stress-strain behavior showing strain hardening, reduced elastic modulus in compression, and Bauschinger effect during initial cycle .....	1
2. Engineering stress-strain plots for A723-1130 MPa pressure vessel .....	2
3. Unloading/reloading experiment on A723-1130 .....	3
4. Comparison of Milligan $\beta$ to the new BSR .....	5
5. Modulus recovery experiment on PH 13-8 ST (1355) .....	6

6.	Life measurements and life prediction of candidate steels.....	9
7.	Life measurements and life prediction of candidate steels with normalized Paris law coefficient and exponent.....	10

## INTRODUCTION

Accurate numerical analyses of stress and strain and, hence, the Bauschinger effect in gun tubes require high quality uniaxial stress-strain data and an accurate numerical fit to such data. These data provide the equivalent stress input to yield criteria such as Von Mises and Tresca for the solution of complex 2D and 3D problems. A detailed overview is given in Lemaitre and Chaboche (ref 1).

The principal features of a uniaxial test for determining Bauschinger effect for gun steels are (see Figure 1):

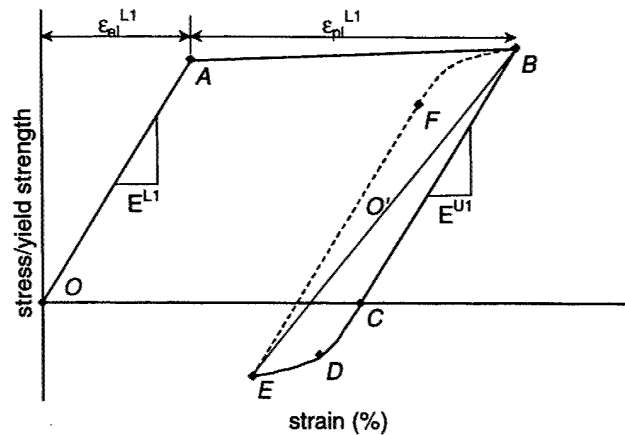


Figure 1. Typical uniaxial stress-strain behavior showing strain hardening, reduced elastic modulus in compression, and Bauschinger effect during initial cycle.

L1: This is an initial tensile loading,  $O-A$ , during which the steel behaves predominantly elastically up to the yield point  $\sigma_Y$  defined by a predetermined percent offset, at a strain level of  $\epsilon_{el}^{L1}$ . The elastic modulus over this range is  $E^{L1}$ . The material then behaves plastically,  $A-B$ , with a very small amount of predominantly linear strain hardening of slope  $S$  over a strain range of  $\epsilon_{pl}^{L1}$ , achieving a maximum tensile stress of  $\sigma_{Y*}$ .

U1: This is a reversal of loading, with the tensile (positive) stress reducing, and subsequently becoming, compressive (negative) at point  $C$  but continuing to behave elastically up to point  $D$  with elastic modulus  $E^{U1}$  over a strain range  $\epsilon_{el}^{U1}$ . Thereafter, behavior becomes non-linear, moving asymptotically towards a stress value of  $(-\sigma_{Y*})$ . The value of stress at point  $D$  is  $-\beta\sigma_Y$ , where  $\beta$  is the traditional Bauschinger effect factor (ref 2). Both  $\beta$  and the shape of the curve  $D-E$  are a strong function of the initial plastic strain  $\epsilon_{pl}^{L1}$ .

L2: This is a further (tensile) strain reversal, producing the type of stress-strain behavior shown as  $E-F-B$ , which approximates to a homothetic transformation of  $B-C-D-E$ , with its center at  $O'$ , the mid-point of  $B-E$  and of  $F-D$ . The value of stress at point  $O'$  is sometimes termed the "back stress."

When a gun tube undergoes autofrettage, the equivalent stress within the gun tube follows *O-A-B* during the initial autofrettage pressurization or swage, and *B-C-D-E* during the removal of swage or pressure. Hence, a family of uniaxial cycles, *O-A-B-C-D-E*, each a function of initial plastic strain and hence of radial location, defines equivalent stress for the gun steel during the autofrettage process. This, in turn, with appropriate equilibrium, compatibility, and boundary conditions, is sufficient to calculate numerically the residual stress locked into the tube by autofrettage. Results of such calculations are well documented for the current range of gun steels (ref 3) and indeed conform extremely well to the ASME PVP code (ref 4).

## EXPERIMENTAL BAUSCHINGER TEST RESULTS

The uniaxial Bauschinger effect has been evaluated in several high-strength steels being considered for armament use. The steels investigated include ASTM A723 (1130 MPa and 1330 MPa), PH 13-8 Mo stainless steel (1380 MPa), PH 13-8 Mo super tough stainless steel (1355 MPa), and HY 180 (1180 MPa). Tests were conducted at plastic strains up to 3.5%.

Uniaxial tension/compression tests were conducted on an Instron Model 1332 servo-hydraulic test machine. Tests were run in strain control at a strain rate of 0.025 mm/mm per s. An extensometer with a full range  $\pm 0.25$  mm, and a total gage length of 25 mm was utilized. The specimen was in a standard 6-mm diameter round tension configuration, with a gage length of five diameters as per ASTM E8 – Standard Test Method for Tension Testing of Metallic Materials. Initial tests were conducted using a unique fixture as described in Mossey et al. (ref 5), whereas later tests were completed with a standard hydraulic wedge grip. The two different grips were compared to assure their similarity, and produced nearly identical stress/strain plots. Fully reversed engineering stress strain plots for each of the materials were made at total strains (elastic strain + plastic pre-strain) of 1, 2, 3 and 4%; and the engineering stress/strain results for the A723-1130 MPa pressure vessel are shown in Figure 2.

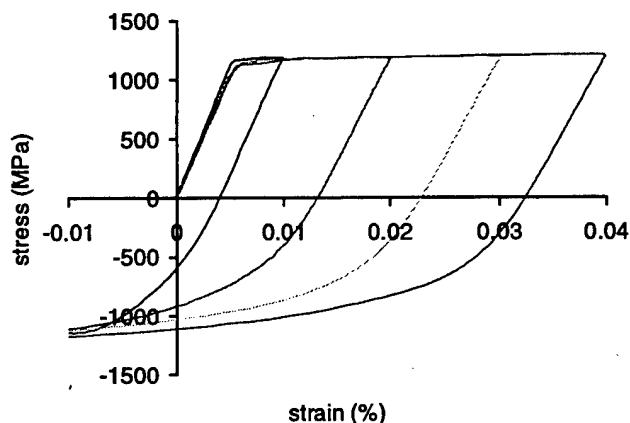


Figure 2. Engineering stress-strain plots for A723-1130 MPa pressure vessel.

## Bauschinger Modulus and Strength Reduction

An interesting feature observed during testing was a reduction in modulus as loading was reversed. This reduction is a strong function of plastic pre-strain. The feature, hereafter termed the Bauschinger Modulus Reduction or BMR ( $= E_{\text{unloading}} / E_{\text{loading}}$ ) can easily be seen in Figure 2 and in Table 1. Note that in the case of A723-1130, the modulus upon unloading is reduced by over 20% at 3.4% plastic pre-strain. In Bauschinger's original work (ref 2), data are presented for several materials, including steel. Bauschinger observed a reduced elastic modulus upon successive reloading after several intervals of increasing plastic strains. No explanation of this phenomenon is given. A repeat of his experiments is presented in Figure 3 for A723-1130. Note the recovery of some of the elastic modulus upon the successive reloads, but the overall trend is towards decreasing elastic modulus with increasing plastic strain, both on the unloading and reloading portion of the cycle. Tests were also conducted initially in compression, and successive unloadings verified that the BMR exists during either tensile or compressive unloadings. The BMR phenomenon is slightly more pronounced when the unloading is tensile, likely the result of changing cross-sectional area effects, which can account for minor differences in compressive versus tensile BMR. It is also unlikely that the BMR is the result of cracking or microvoid coalescence, as it occurs on the first unloading, after even the smallest amount of plastic pre-strain.

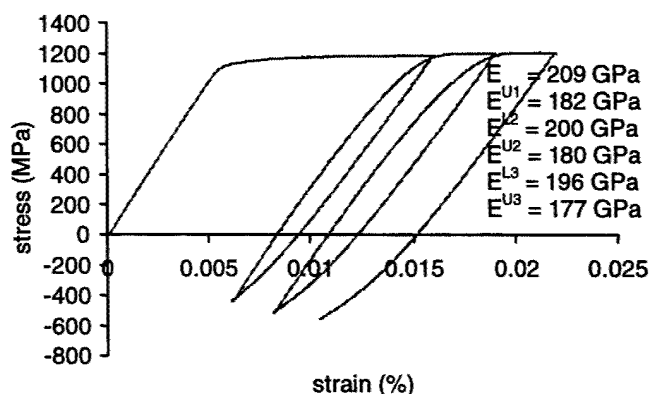


Figure 3. Unloading/reloading experiment on A723-1130.

Puskar (ref 6) describes the BMR phenomenon as a four-stage event. Stage 1 involves an applied pre-strain amplitude, which is too small to result in any dislocation movement, where  $E_{\text{unloading}} = E_{\text{loading}}$ . Stage 2 is a result of a redistribution of locking point and an increase in the effective dislocation length as the applied pre-strain increases past a critical Stage 1 point. The result is  $E_{\text{Stage 2}} < E_{\text{loading}}$ . In Stage 3, increased applied pre-strain amplitude results in the generation of dislocations. These changes in the dislocation density result in significant changes in the physical and mechanical properties of the material, and hence  $E_{\text{Stage 3}} < E_{\text{Stage 2}}$ . During Stage 4, the further increased applied pre-strain amplitude results in damage and a further reduction in the modulus or  $E_{\text{Stage 4}} < E_{\text{Stage 3}}$ . The four stages are functions of many factors, including material type, composition, processing, etc. Each of the stages need not occur



simultaneously, or in fact be present under all sets of conditions. They can overlap at various intervals within the structure and the resultant BMR can indeed be a continuous smooth curve when plotted against the applied plastic pre-strain amplitude.

A second interesting feature observed from testing is the deviation from the unloading modulus, which begins when the specimen goes into reverse loading after prior plastic pre-straining. This deviation (in A723 1130), for normal amounts of plastic pre-strain from 0 to 1.4%, and relative compressive strain from 0 to 1%, is virtually independent of plastic pre-strain and depends only on compressive strain. For plastic pre-strain greater than about 1.4%, the deviation is a relatively weak function of plastic pre-strain. All materials investigated exhibit this deviation from linear behavior, with saturation occurring in all materials between 1 and 2% plastic pre-strain. This feature is hereafter termed the Bauschinger Strength Reduction or BSR is calculated at the point of linear deviation as  $BSR = \sigma_{\text{deviation}} / \sigma_{\text{yield}}$ . In the traditional sense of the term  $\beta$  is calculated the same way as is BSR. They are, however, different because  $\beta$  follows an unloading path equal to  $E_{\text{unloading}} = E_{\text{loading}}$ , whereas BSR follows a reduced unloading path that depends on the amount of prior plastic pre-straining, or  $E_{\text{unloading}} = BMR \times E_{\text{loading}}$ .

**Table 1. Bauschinger Test Data**

Material	$\epsilon_{\text{total}}$	$\epsilon_{\text{plastic}}$	Modulus (GPa)		BMR	BSR		
			loading	unloading		0.05%	0.10%	0.20%
A723-1130	1.00	0.48	219	201	0.917	-0.284	-0.511	-0.666
	2.00	1.45	202	174	0.863	-0.240	-0.363	-0.490
	3.00	2.45	204	166	0.813	-0.276	-0.392	-0.505
	4.00	3.45	202	161	0.798	-0.230	-0.355	-0.477
A723-1330	1.00	0.36	208	192	0.925	-0.552	-0.677	-0.830
	2.00	1.27	208	182	0.874	-0.200	-0.333	-0.474
	3.00	2.40	208	170	0.819	-0.216	-0.338	-0.464
	4.00	3.26	207	167	0.808	-0.123	-0.273	-0.418
PH 13-8-ST-1355	1.00	0.33	197	187	0.953	-0.494	-0.678	-0.919
	2.00	1.32	193	165	0.852	-0.264	-0.391	-0.530
	3.00	2.33	196	165	0.842	-0.255	-0.380	-0.514
	4.00	3.33	196	162	0.827	-0.247	-0.378	-0.514
PH 13-8-1380	1.00	0.31	196	186	0.948	-0.559	-0.742	-0.980
	2.00	1.32	200	175	0.876	-0.285	-0.404	-0.539
	3.00	2.31	198	165	0.835	-0.290	-0.394	-0.515
	4.00	3.34	208	164	0.788	-0.296	-0.420	-0.551
HY 180-1180	2.00	1.39	190	169	0.888	-0.529	-0.609	-0.692
	3.00	2.45	181	155	0.857	-0.356	-0.459	-0.578
	4.00	3.41	191	153	0.804	-0.384	-0.476	-0.574

The pertinent data for the investigated materials can be seen in Table 1, with BSR presented for 0.05, 0.10, and 0.20% offsets.

### Comparison to Milligan Data

Prior work relating to the Bauschinger effect on gun steels was somewhat limited. Work by Milligan et al. (ref 7) provided some indication of  $\beta$  for an early vintage A723 gun steel (1100 MPa). Their publication was somewhat incomplete in that no traces of their stress/strain plot were provided. Comparison of Milligan's  $\beta$  to that generated here (BSR) provided good agreement, as seen in Figure 4.

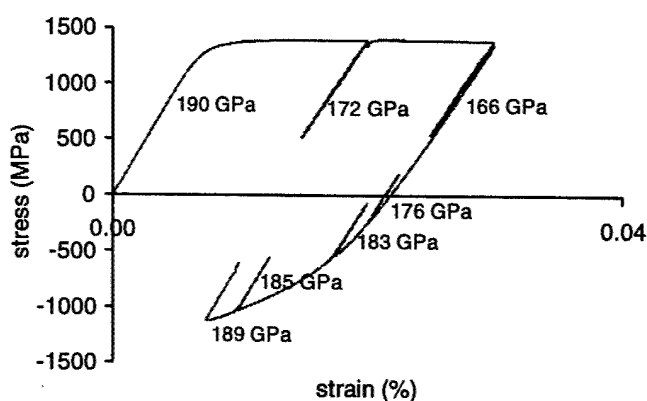


Figure 4. Comparison of Milligan  $\beta$  to the new BSR.

### Modulus Recovery

Tests were conducted to investigate modulus recovery effects. For each of the materials investigated, a multiple loading experiment was conducted where the specimens were loaded in tension at several prescribed plastic pre-strain levels. At each strain level, an unloading and reloading were conducted. The specimen was then loaded into compression and the unloadings and reloadings were repeated. Figure 5 shows the test conducted on PH 13-8 ST 1355. Observe the reduction in modulus during the tensile unloading and reloading, and the recovery of modulus during the compressive unloading and reloading. This apparent recovery of modulus suggests that some of the stages identified in Puskar's analysis are indeed reversible. It is likely that Stages 1 and 2 in Puskar's hypothesis are reversible, because no dislocations are as of yet generated; and Stages 3 and 4 are believed to be irreversible. It is not known, nor was it the objective of this paper to investigate, at which point irreversible damage had occurred. For the plastic strains of the order of magnitude investigated here, the sample materials exhibited considerable recovery of elastic modulus.

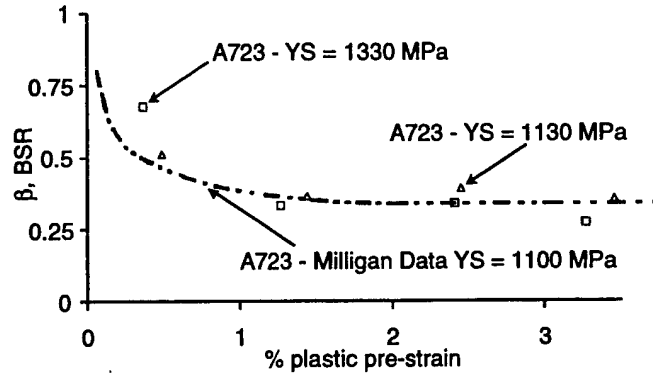


Figure 5. Modulus recovery experiment on PH 13-8 ST (1355).

## ANALYSIS OF RESIDUAL STRESSES/ NUMERICAL FIT OF THE BAUSCHINGER EFFECT

Pressure vessels are often autofrettaged to impart favorable compressive residual stresses at their bores. These compressive residual stresses are largest at the bore and act to resist crack initiation and subsequent crack propagation. Historically, these residual stresses were approximated using approaches such as that presented in Hill (ref 8). Hill's approach accounted only for closed-ended pressure vessels, and does not consider the Bauschinger effect. Recent work published by Parker (ref 3) has taken the classical approach further, to include the Bauschinger effect, for a typical pressure vessel steel, and open-ended pressure vessels. Parker and Underwood further improve this work (ref 10) to include the Bauschinger effect on several different candidate pressure vessel steels. The analysis presented in by Parker (ref 3) utilized the uniaxial engineering stress/strain data presented here for the candidate materials.

Calculation of the autofrettage residual stress at the bore of a pressure vessel, as determined by a Tresca plane stress analysis without Bauschinger effect, is given by

$$\sigma_{\theta-\text{bore}}^T = Y[(c^2 - a^2) - 2b^2 \ln(c/a)]/(b^2 - a^2) \quad (1)$$

where  $Y$  is the material yield strength,  $a$  is the bore radius,  $b$  is the outside radius, and  $c$  is the elastic/plastic autofrettage radius or

$$c = (b - a) \times m + a \quad (2)$$

where  $m$  is the percent autofrettage. The residual stress, which accounts for Bauschinger effects for A723 pressure vessel steel (at 1100 MPa) and is valid on the range  $c/a \leq 2.22$  and  $30\% \leq m \leq 80\%$  and can be determined by

$$\sigma_{\theta-\text{bore}} = R_s \sigma_{\theta-\text{bore}}^T \quad (3)$$

where

$$R_s = 1.669 - 0.1651 (b/a) - 0.730 m^3 + 1.984 m^2 - 1.887 m \quad (4)$$

The hoop residual stress at the bore of a pressure vessel, which includes the Bauschinger effect and open-ended conditions for the various materials investigated, can then be determined by

$$\sigma_{\theta\text{-bore}}^R = \gamma \sigma_{\theta\text{-bore}} \quad (5)$$

where the scaling factor  $\gamma$  takes the form

$$\gamma = 1 / \{ [A(b/a) + B] \text{EXP} \{ [C(b/a) + D][(c/a) + E] \} + [F(b/a) + G] \} \quad (6)$$

for the two A723 materials and the two PH 13-8 alloys; the constants in equation (6) are presented in Table 2.

**Table 2. Bauschinger Scaling Factor Constants**

	A723 1130	A723 1330	PH 13-8 Mo-1380	PH 13-8 Mo (ST) 1355
<b>A</b>	0.0816	0.1276	0.1635	0.1685
<b>B</b>	-0.0562	-0.1737	-0.0828	-0.1039
<b>C</b>	1.7519	-0.3911	0.3193	1.2539
<b>D</b>	-7.4597	-1.0484	-3.2164	-5.8889
<b>E</b>	-1.315	-1.322	-1.472	-1.470
<b>F</b>	-0.1077	-0.0927	-0.1483	-0.1655
<b>G</b>	1.216	1.1642	1.2424	1.2875
Valid Range	$c/a \geq 1.5$ $b/a \geq 1.75$	$c/a \geq 1.5$ $b/a \geq 1.75$	$c/a \geq 1.5$ $b/a \geq 1.75$	$c/a \geq 1.5$ $b/a \geq 1.75$

For HY 180-1180 the scaling factor  $\gamma$  takes the form

$$\gamma = [-0.0506(b/a) + 0.0178](c/a) + 0.0944(b/a) + 0.9611 \quad (7)$$

which is also valid in the range  $c/a \geq 1.5$  and  $b/a \geq 1.75$ . The scaling factor  $\gamma$  accounts for the BMR, BSR, and for open-ended pressure vessel conditions.

## FATIGUE LIFE APPROXIMATION

The Paris law accurately describes the fatigue crack growth of many materials. In many situations, it has successfully been utilized to predict fatigue crack propagation (Stage II cracking), and final failure (Stage III cracking). Since gun tubes are typically field fired prior to laboratory fatigue cycling, Stage I or crack initiation is not an issue. This field firing prior to lab

cycling can lead to some error in approximating life, as damage as a result of this firing can lead to inconsistent initial crack depths, and, hence, life measurements can exhibit large amounts of scatter. The Paris law is well recognized as

$$d\bar{a}/dN = C' \Delta K^n \quad (8)$$

where  $C'$  and  $n$  are experimental constants (defined in Table 3) and  $\Delta K$ , the range of stress intensity, is defined as

$$\Delta K = \Delta\sigma (\pi\bar{a})^{1/2} \quad (9)$$

where  $\bar{a}$  is the crack depth and  $\Delta\sigma$  reflects the positive range of the sum of the Lamé hoop stress and Bauschinger corrected residual hoop stress at the bore, or

$$\Delta\sigma = \Delta\sigma_{\text{Lame}} + \sigma_{\theta-\text{bore}}^R \quad (10)$$

Once equations (9) and (10) are input into equation (8), and equation (8) is integrated, the Paris Law takes the form

$$N = [1/(C' \pi^{n/2} (1 - n/2) \Delta\sigma^n)] [a_f^{1-n/2} - a_o^{1-n/2}] \quad (11)$$

where  $N$  represents the total life and  $a_f$  and  $a_o$  represent the final and initial crack length, respectively.

**Table 3. Paris Law Coefficients and Exponents**

	A723 1130	A723 1330	PH 13-8 Mo 1380	PH 13-8 Mo (ST) 1355	HY 180 1180
$C'$ (E-11m/cycle)	2.41	6.05	0.759	0.759	9.48
$n$	2.80	2.44	2.87	2.87	2.30

Parker and Underwood (ref 10) have studied the effect of fatigue lives, which they have corrected for the Bauschinger effect using the Milligan data for A723 steel for a specific set of non-autofrettagged and 50% autofrettagged pressure vessels. This current work will take their analysis further and approximate lives for all of the materials studied. Assuming a  $b/a$  of 1.88, a firing pressure of 670 MPa, initial crack length  $a_o$  of 0.0001 m (typical of a pre-fired cannon tube), and a final crack length  $a_f (= b - a)$  of 0.069 m, we may approximate the lives as a function of the percent autofrettage. Results for each of the materials are presented in Figure 6. Note in the figure that there is a general trend for a dimensioning return on life of the pressure vessels as the percent autofrettage is increased for the A723 steels, PH 13-8 Mo steels (which have been lumped together because they essentially follow the same curve), and the HY 180. Also note that although the Milligan data are not shown, there is generally good agreement on life when compared to the new data presented here for A723 1130 MPa. Differences of less than 12% over the full range of autofrettage are observed, and the general shapes of the two curves are nearly identical. As expected, the predicted lives are more for the ASTM A723 1330, PH 13-8 Mo

alloys and HY 180 1180 over those predicted for the A723 1130; this results from a combination of increases in strength and differential fatigue crack growth behavior. For a given overstrain, a higher strength material will always produce higher compressive residual stresses, which, in turn, will result in longer lives if fatigue crack growth behavior is the same for each material (i.e., Paris law coefficients are unchanged between materials). Incorporating differential fatigue crack growth behavior may increase or decrease these differences in lifetime. In Figure 6 are seven laboratory fatigue test results for A723 1130 MPa pressure vessels meeting the previously defined conditions for 65 to 75% autofrettage. The tests are in good agreement with those predicted; however, the predictions on life are conservative when compared to the new test data. This is likely the result of the pre-fatigue test damage to the bore surface being larger than the 0.0001 m used in the predictive model.

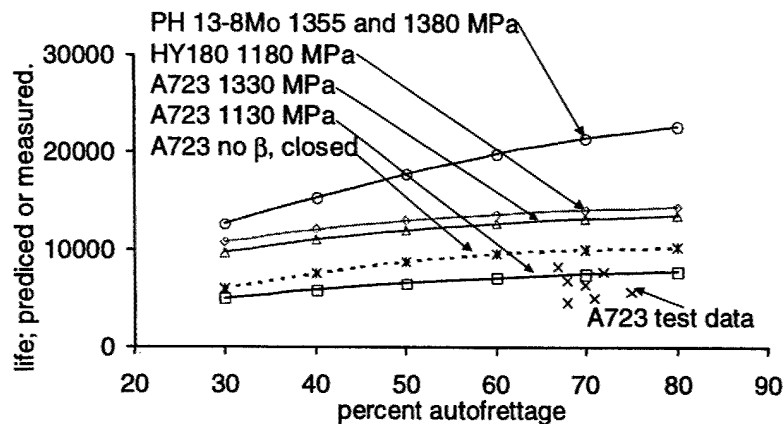


Figure 6. Life measurements and life prediction of candidate steels.

To investigate the effects of Paris law coefficients on fatigue life, an analysis that normalized these inputs to those of A723 1130 MPa steel was conducted. All of the materials investigated were assumed to have the same  $C'$  and  $n$  as the A723 1130 MPa steel, with all other input variables as previously defined, including the amount of residual stress as predicted by equation (5). The results of the analysis were quite staggering (Figure 7) and suggest that the controlling factor in estimating fatigue life is not the increase in strength, which controls the amount of compressive residual stresses that the pressure vessel is capable of, but is the Paris law coefficients, which are the single most controlling factor in predicting fatigue lives.

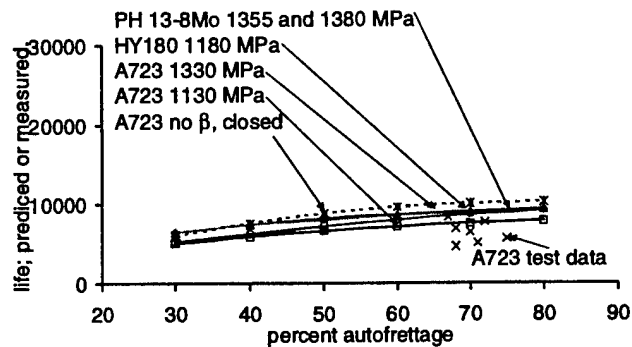


Figure 7. Life measurements and life prediction of candidate steels with normalized Paris law coefficient and exponent.

## CLOSING REMARKS

Uniaxial stress-strain experiments have been conducted on several candidate pressure vessel steels, including A723, PH 13-8 Mo and HY 180 in an attempt to evaluate the loss of compressive residual stress as a result of prior plastic tensile straining, also known as the Bauschinger effect. The utilization of these data has led to the following observations and conclusions.

- In the class of pressure vessel steels investigated here, a trend of decreased unloading modulus was observed after prior plastic pre-straining. The decreasing unloading modulus, termed the Bauschinger Modulus Reduction, BMR, was shown to continue to decrease as the amount of plastic pre-straining increases.
- The Bauschinger Strength Reduction, BSR, is the reduced compressive strength after plastic pre-straining, and follows the BMR unloading slope. The BSR saturates between 1 and 2% for all material investigated, after which point no further decrease in BSR is observed.
- The BSR test results compare favorably with the Bauschinger results published by Milligan et al. (ref 7) for A723 steel.
- Parker et al. (ref 9) have used the test data generated here to numerically predict the effects of the loss of compressive residual hoop stress at the bore of an autofrettaged pressure vessel. The analysis not only takes into account the loss of stresses attributable to the Bauschinger effect, but also for an open-ended pressure vessel.
- The residual stress results are utilized to predict fatigue lives that take into account both the Bauschinger effect (including the BSR and BMR) and open-ended pressure vessel conditions. These predicted life results compare favorably with those measured in actual full-scale A723 pressure vessel fatigue tests.

- All things being equivalent, it appears that the Paris Law coefficients  $C'$  and  $n$  are the single most influencing factor when approximating fatigue lives.



## REFERENCES

1. Lemaitre, J., and Chaboche, J.L., *Mechanics of Solid Materials*, Cambridge University Press, 1990.
2. Bauschinger, J., "Ueber die Veränderung der Elasticitätsgrenze und dea Elasticitätsmoduls verschiadener Metalle," *Zivilingenieur*, Vol. 27, 1881, Columns 289-348.
3. Parker, A.P., "Autofrettage of Open-End Tubes – Pressures, Stresses, Strains and Code Comparisons," *Trans. ASME, J. Pressure Vessel Technology*, Vol. 123, pp. 271-281.
4. "Design Using Autofrettage," *ASME Pressure Vessel and Piping Design Code*, Division 3, Section 8, Article KD-5, 1997, pp. 71-73.
5. Mossey, C., Troiano, E., and Pfindl, F., "Bauschinger Test Fixture," ARDEC Memorandum Report ARCCB-MR-03001, Benet Laboratories, Watervliet, NY, February 2003.
6. Puskar, A., "A Correlation Among Elastic Modulus Defect, Plastic Strain and Fatigue Life of Metals," *Materials Science Forum*, Vol. 119-121, 1993, pp. 455-460.
7. Milligan, R.V., Koo, W.H., and Davidson, T.E., "The Bauschinger Effect in a High Strength Steel," *Trans. ASME, D*, 1966, pp. 480-488.
8. Hill, R., *The Mathematical Theory of Plasticity*, Oxford University Press, Oxford, UK, 1967.
9. Parker, A.P., Troiano, E., Underwood, J.H., and Mossey, C., "Characterization of Steels Using a Revised Kinematic Hardening Model Incorporating Bauschinger Effect," ARDEC Technical Report ARCCB-TR-02009, Benet Laboratories, Watervliet, NY, August 2002.
10. Parker, A.P., and Underwood, J.H., "Influence of the Bauschinger Effect on Residual Stress and Fatigue Lifetimes in Autofrettaged Thick-Walled Cylinders," *Fatigue and Fracture Mechanics*, 29<sup>th</sup> Vol. *ASTM STP 1321*, (T.L. Panontin and S.D. Sheppard, eds.), 1998.

---

TECHNICAL REPORT INTERNAL DISTRIBUTION LIST

	<u>NO. OF COPIES</u>
TECHNICAL LIBRARY ATTN: AMSTA-AR-CCB-O	1
TECHNICAL PUBLICATIONS & EDITING SECTION ATTN: AMSTA-AR-CCB-O	3
PRODUCTION PLANNING & CONTROL DIVISION ATTN: AMSTA-WV-ODP-Q, BLDG. 35	1

NOTE: PLEASE NOTIFY DIRECTOR, BENÉT LABORATORIES, ATTN: AMSTA-AR-CCB-O OF ADDRESS CHANGES.

---

---

TECHNICAL REPORT EXTERNAL DISTRIBUTION LIST

	<u>NO. OF COPIES</u>		<u>NO. OF COPIES</u>
DEFENSE TECHNICAL INFO CENTER		COMMANDER	
ATTN: DTIC-OCA (ACQUISITIONS)	2	U.S. ARMY RESEARCH OFFICE	
8725 JOHN J. KINGMAN ROAD		ATTN: TECHNICAL LIBRARIAN	1
STE 0944		P.O. BOX 12211	
FT. BELVOIR, VA 22060-6218		4300 S. MIAMI BOULEVARD	
		RESEARCH TRIANGLE PARK, NC 27709-2211	
COMMANDER		COMMANDER	
U.S. ARMY ARDEC		ROCK ISLAND ARSENAL	
ATTN: AMSTA-AR-WEE, BLDG. 3022	1	ATTN: SIORI-SEM-L	1
AMSTA-AR-AET-O, BLDG. 183	1	ROCK ISLAND, IL 61299-5001	
AMSTA-AR-FSA, BLDG. 61	1		
AMSTA-AR-FSX	1	COMMANDER	
AMSTA-AR-FSA-M, BLDG. 61 SO	1	U.S. ARMY TANK-AUTMV R&D COMMAND	
AMSTA-AR-WEL-TL, BLDG. 59	2	ATTN: AMSTA-DDL (TECH LIBRARY)	1
PICATINNY ARSENAL, NJ 07806-5000		WARREN, MI 48397-5000	
DIRECTOR		COMMANDER	
U.S. ARMY RESEARCH LABORATORY		U.S. MILITARY ACADEMY	
ATTN: AMSRL-DD-T, BLDG. 305	1	ATTN: DEPT OF CIVIL & MECH ENGR	1
ABERDEEN PROVING GROUND, MD		WEST POINT, NY 10966-1792	
21005-5066			
DIRECTOR		U.S. ARMY AVIATION AND MISSILE COM	
U.S. ARMY RESEARCH LABORATORY		REDSTONE SCIENTIFIC INFO CENTER	2
ATTN: AMSRL-WM-MB (DR. B. BURNS)	1	ATTN: AMSAM-RD-OB-R (DOCUMENTS)	
ABERDEEN PROVING GROUND, MD		REDSTONE ARSENAL, AL 35898-5000	
21005-5066			
CHIEF		NATIONAL GROUND INTELLIGENCE CTR	
COMPOSITES & LIGHTWEIGHT STRUCTURES		ATTN: DRXST-SD	
WEAPONS & MATLS RESEARCH DIRECT	1	2055 BOULDERS ROAD	1
U.S. ARMY RESEARCH LABORATORY		CHARLOTTESVILLE, VA 22911-8318	
ATTN: AMSRL-WM-MB (DR. BRUCE FINK)			
ABERDEEN PROVING GROUND, MD 21005-5066			

---

NOTE: PLEASE NOTIFY COMMANDER, ARMAMENT RESEARCH, DEVELOPMENT, AND ENGINEERING CENTER,  
 BENÉT LABORATORIES, CCAC, U.S. ARMY TANK-AUTOMOTIVE AND ARMAMENTS COMMAND,  
 AMSTA-AR-CCB-O, WATERVLIET, NY 12189-4050 OF ADDRESS CHANGES.

---